Atherosclerosis 375 (2023) 21–29

Contents lists available at ScienceDirect

Atherosclerosis

journal homepage: www.elsevier.com/locate/atherosclerosis

Hepatic *Cdkal1* deletion regulates HDL catabolism and promotes reverse cholesterol transport

Dan Bi An [a,1], Soo-jin Ann [b,1], Seungmin Seok [a], Yura Kang [c], Sang-Hak Lee [d,e,*]

[a] Yonsei University Graduate School, Seoul, South Korea
[b] Integrative Research Center for Cerebrovascular and Cardiovascular Diseases, Yonsei University College of Medicine, Seoul, South Korea
[c] Department of Biostatistics and Computing, Yonsei University Graduate School, Seoul, South Korea
[d] Division of Cardiology, Department of Internal Medicine, Yonsei University College of Medicine, Seoul, South Korea
[e] Pohang University of Science and Technology (POSTECH), Pohang, South Korea

ARTICLE INFO

Keywords:
Genetics
Lipoproteins
Coronary artery disease
Drug development

ABSTRACT

Background and aims: Associations between *CDKAL1* variants and cholesterol efflux capacity (CEC) have been reported. This study aimed to investigate the effects of Cdkal1 deficiency on high-density lipoprotein (HDL) metabolism, atherosclerosis, and related pathways.

Methods: Lipid and glucose metabolic profiles, CEC, and *in vivo* reverse cholesterol transport (RCT) were compared in liver-specific *Alb-Cre:Cdkal1*$^{fl/fl}$ and *Cdkal1*$^{fl/fl}$ mice. Aortic atherosclerosis was compared in *Apoe*$^{-/-}$*Alb-Cre:Cdkal1*$^{fl/fl}$ and *Apoe*$^{-/-}$ mice fed high-fat diets. HDL subclasses and mediators of HDL metabolism from *Alb-Cre:Cdkal1*$^{fl/fl}$ mice were examined.

Results: HDL-cholesterol level tended to be higher in the *Alb-Cre:Cdkal1*$^{fl/fl}$ mice ($p = 0.050$). Glucose and other lipid profiles were similar in the two groups of mice, irrespective of diet. The mean CEC was 27% higher ($p = 0.007$) in the *Alb-Cre:Cdkal1*$^{fl/fl}$ mice, as were the radioactivities of bile acids (mean difference 17%; $p = 0.035$) and cholesterol (mean difference 42%; $p = 0.036$) from faeces. The radioactivity tendency was largely similar in mice fed a high-fat diet. Atherosclerotic lesion area tended to be smaller in the *Apoe*$^{-/-}$*Alb-Cre:Cdkal1*$^{fl/fl}$ mice than in the *Apoe*$^{-/-}$ mice ($p = 0.067$). Cholesterol concentrations in large HDLs were higher in the *Alb-Cre:Cdkal1*$^{fl/fl}$ mice ($p = 0.024$), whereas in small HDLs, they were lower ($p = 0.024$). Endothelial lipase (mean difference 39%; $p = 0.002$) and hepatic lipase expression levels (mean difference 34%; $p < 0.001$) were reduced in the *Alb-Cre:Cdkal1*$^{fl/fl}$ mice, whereas SR-B1 expression was elevated (mean difference 35%; $p = 0.007$).

Conclusions: The promotion of CEC and RCT in *Alb-Cre:Cdkal1*$^{fl/fl}$ mice verified the effect of *CDKAL1* seen in human genetic data. These phenotypes were related to regulation of HDL catabolism. This study suggests that *CDKAL1* and associated molecules could be targets for improving RCT and vascular pathology.

1. Introduction

In traditional studies, the relationship between low high-density lipoprotein-cholesterol (HDL-C) levels and coronary heart disease risk has been well reported [1,2]. However, following genetic studies [3] and trials of HDL-C raising drugs [4], there is further uncertainty on whether HDL is protective against atherosclerosis or if HDL-C is just a biomarker. Conversely, very recent genetic studies analysing characteristics of HDL particles revealed a protective effect against coronary artery disease [5]. Furthermore, many researchers and physicians are still interested in the influence of therapeutics based on HDL and reverse cholesterol transport (RCT) on vascular disease [6,7].

We previously reported associations between variants of *CDKAL1*, encoding Cdk5 regulatory subunit associated protein 1-like 1 (Cdkal1), and cholesterol efflux capacity (CEC) using a human genome-wide association and replication study. In that study, 631 variants were associated in the discovery set, and five of these, including four near *CDKAL1*, were associated with CEC in the replication set [8]. Based on these results, we planned to investigate the pathways by which *Cdkal1* affects CEC and whether this gene influences RCT and atherosclerosis.

* Corresponding author. Division of Cardiology, Department of Internal Medicine, Yonsei University College of Medicine, 134 Shinchon-dong, Seodaemun-gu, Seoul, 120-752, South Korea.
E-mail address: shl1106@yuhs.ac (S.-H. Lee).
[1] These two authors contributed equally to this work.

https://doi.org/10.1016/j.atherosclerosis.2023.05.012
Received 19 September 2022; Received in revised form 13 May 2023; Accepted 16 May 2023
Available online 22 May 2023

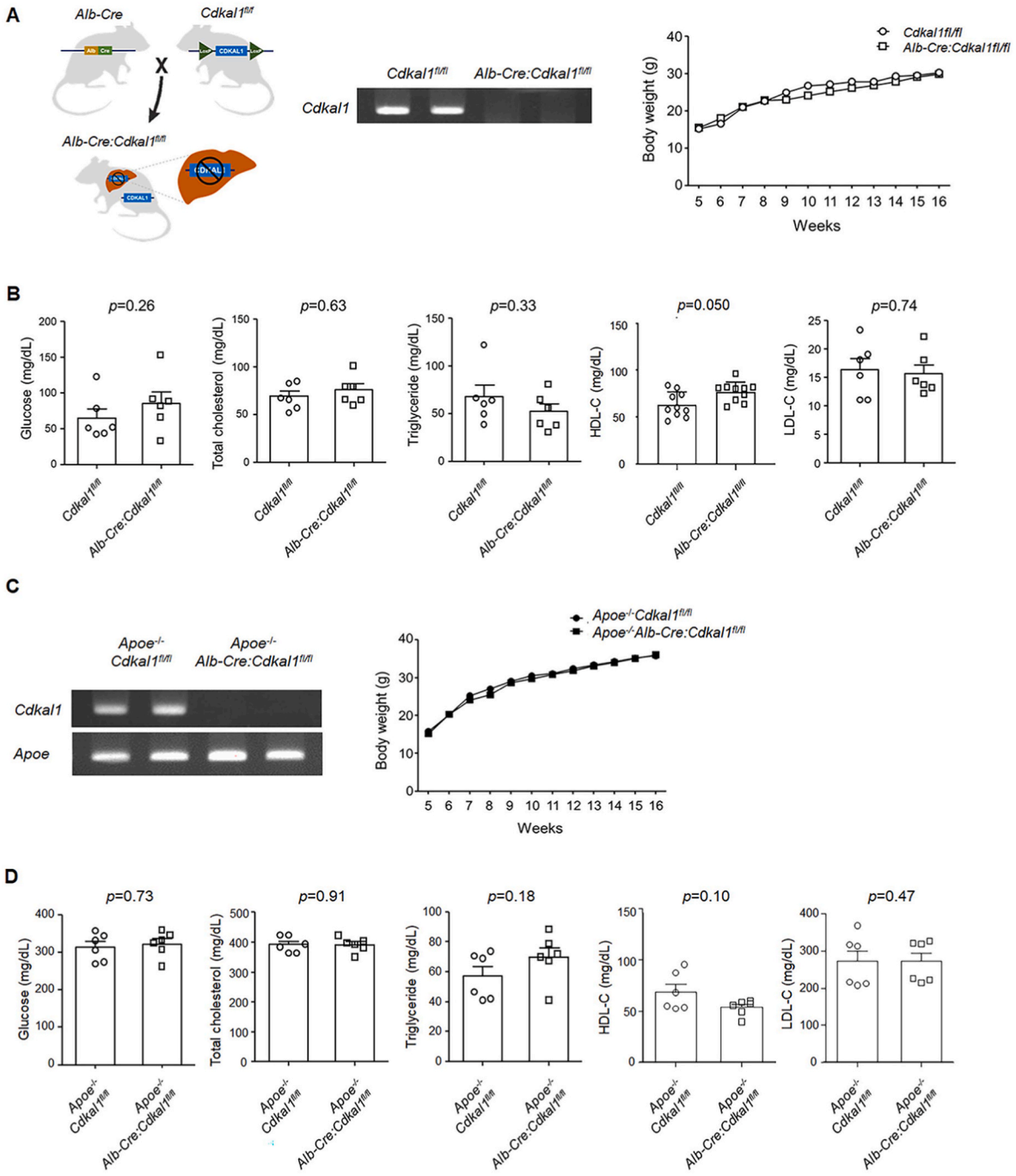

Fig. 1. Generation and basic characteristics of liver-specific Cdkal1-deficient mice.
(A) Schematic illustration of the generation of liver-specific Cdkal1-deficient mice. Mice with floxed alleles were bred with those expressing Cre recombinase to produce tissue-specific *Alb-Cre*:*Cdkal1*$^{fl/fl}$ mice (left panel). PCR amplification of excised genomic region containing *Cdkal1* in the liver of *Alb-Cre*:*Cdkal1*$^{fl/fl}$ mice (middle panel). Body weight of male *Cdkal1*$^{fl/fl}$ and *Alb-Cre*:*Cdkal1*$^{fl/fl}$ mice fed a chow diet (right panel) (p = not significant; permutation test; n = 12 in each group). (B) Circulating levels of glucose and lipids of male *Cdkal1*$^{fl/fl}$ mice and *Alb-Cre*:*Cdkal1*$^{fl/fl}$ mice fed a chow diet (p = not significant for all variables; permutation test; n = 6–10 in each group). (C) Production and genotyping of *Apoe*$^{-/-}$*Alb-Cre*:*Cdkal1*$^{fl/fl}$ mice. DNA was amplified with primers for *Cdkal1* (350 bp) and *Apoe* (220 bp). PCR products were separated on 6% agarose gels (left panel). Comparison of body weights of male *Apoe*$^{-/-}$ and *Apoe*$^{-/-}$*Alb-Cre*:*Cdkal1*$^{fl/fl}$ mice (fed with high-fat diets for 16 weeks; right panel) (p = not significant; permutation test; n = 12 in each group). (D) Circulating levels of glucose and lipids of male *Apoe*$^{-/-}$ and *Apoe*$^{-/-}$*Alb-Cre*:*Cdkal1*$^{fl/fl}$ mice (fed with high-fat diets for 16 weeks) (p = not significant for all variables; permutation test; n = 6 in each group). Data are presented as the mean ± standard error of the mean.

In prior studies, genetic variants of *Cdkal1* were linked to impaired insulin response and the risk of type 2 diabetes mellitus in diverse ethnic populations [9]. As a mammalian methylthiotransferase, Cdkal1 has been reported to catalyse modification of tRNA needed in protein translation [10]. Mice with β cell-specific knockout of Cdkal1 showed a decrease in proinsulin secretion with impaired blood glucose control. This might be due to the low translational efficiency of hypomodified tRNA that causes reduction of proinsulin synthesis [10]. However, no study to date has reported its effects on HDL metabolism or related parameters.

Therefore, the aim of this study was to investigate the effect of Cdkal1 deficiency associated with CEC on HDL metabolism as well as atherosclerosis and its underlying mechanisms. Liver-specific Cdkal1-deficient mice were generated, and lipid profiles, CEC, and RCT were compared in *Alb-Cre*:*Cdkal1*$^{fl/fl}$ and *Cdkal1*$^{fl/fl}$ mice. As mentioned above, a strong metabolic phenotype has been reported in mice with β-cell specific Cdkal1 deletion. However, as the liver plays important roles in HDL metabolism and RCT [11], we used liver-specific knockout mice in the current study. In addition, aortic atherosclerosis was compared in *Apoe*$^{-/-}$*Alb-Cre*:*Cdkal1*$^{fl/fl}$ and *Apoe*$^{-/-}$ mice fed high-fat diets. To elucidate associated biological pathways, regulatory effects on target molecules involved in HDL metabolism were assessed.

2. Materials and methods

2.1. Animals and cells

Liver-specific Cdkal1-deficient mice were generated by crossing *Cdkal1*$^{fl/fl}$ mice (gifted by Prof. Tomizawa of Kumamoto University, Kumamoto, Japan) with albumin Cre recombinase transgenic mice (The Jackson Laboratory, Bar Harbor, ME, USA; Fig. 1A). *Apoe*$^{-/-}$*Alb-Cre*:*Cdkal1*$^{fl/fl}$ mice were generated by crossing *Alb-Cre*:*Cdkal1*$^{fl/fl}$ mice with *Apoe*$^{-/-}$ mice (The Jackson Laboratory; Fig. 1B). All mice were maintained in a controlled environment with a 12-h light/dark cycle (dark cycle: 6 p.m. to 6 a.m.) at 22 °C in individually ventilated cages. Mice were provided free access to standard chow and water. Only male mice were used for all experiments in the current study. Biological sex is one of the key factors for atherosclerosis, and oestrogen is known to influence pathways in lipid metabolism [12]. To minimize sex-related bias, we decided to use male mice only.

For evaluation of aortic atherosclerosis, 5-week-old *Apoe*$^{-/-}$ and *Apoe*$^{-/-}$*Alb-Cre*:*Cdkal1*$^{fl/fl}$ mice were fed high-fat diets (16% fat, 1.25% cholesterol, and 0.5% cholic acid [wt/wt]) for 16 weeks. Mouse aortas were harvested after carefully removing the surrounding fat and connective tissue. After being dissected longitudinally and fixed in 4% (wt/v) paraformaldehyde, the aortas were stained with Oil Red O [60% (v/v) in isopropanol] and pinned for en face preparation. Aorta images were obtained with a light microscope camera, and atherosclerotic areas were measured using ImageJ (NIH, Bethesda, MD, USA). All animal experiments were approved by our local Institutional Animal Care and Use Committee (2017-0307). All animal procedures conformed to the guidelines from Directive 2010/63/EU of the European Parliament on the protection of animals used for scientific purposes. Mice were euthanized by isoflurane anesthesia (5% isoflurane-air mixture).

J774 macrophages were provided by Prof. Yury Miller of the University of California San Diego (La Jolla, CA, USA). J774 cells were cultured in Dulbecco's modified Eagle's medium supplemented with 10% foetal bovine serum at 37 °C in 5% CO_2.

2.2. Measurement of blood metabolic parameters and polymerase chain reaction (PCR)

After overnight fast, blood samples were collected from the abdominal vena cava, and the samples were allowed to clot for 30 min at room temperature before separation by centrifugation (3000 rpm for 30 min at 4 °C). The levels of glucose, total cholesterol, triglyceride, HDL-C, and low-density lipoprotein-cholesterol were measured using an automatic biochemical analyzer (Konelab PRIME 60i, Thermo Fisher Scientific, Waltham, MA, USA). Glucose oxidase-peroxidase, cholesterol oxidase, enzymatic trinder, and direct methods were used, respectively, to assay each of these components. For PCR, DNA was isolated from tissues using a Phire animal tissue direct PCR kit, and PCR was conducted under specific conditions according to the primers (Supplementary Table 1). Then, genotyping was performed by electrophoresis on 4% agarose gel.

2.3. CEC assay

CEC was determined using the following method: J774 cells (RRID: CVDL_0358: passage number 20–29) were plated on 24-well plates at a density of 4×10^4 cells/well and radiolabelled with ^{3}H-cholesterol (2 μCi/well) for 24 h. For the upregulation of adenosine triphosphate-binding cassette transporter subfamily member A1, cells were incubated with medium containing 0.2% bovine serum albumin and 0.3 mmol/L 8-(4-chlorophenylthio)-cyclic adenosine monophosphate for 6 h, as described previously [13]. The cells were then washed once with phosphate-buffered saline (PBS) and incubated in medium containing 5% diluted apoB-depleted serum at 37 °C for 4 h [14]. Serum for CEC assay was obtained from each animal. After overnight fasting, the blood samples were collected and prepared as mentioned in the preceding paragraph. The assay was conducted by treating the cells with 2 mg/mL acyl-coenzyme A:cholesterol acyl transferase inhibitor. The radioactivities of both the medium and cells were then measured. CEC was calculated as: {^{3}H-cholesterol (μCi) in medium/[^{3}H-cholesterol (μCi) in medium + ^{3}H-cholesterol (μCi) in cells]} × 100. The background value was subtracted from all sample values. The values were adjusted based on the CEC of the pooled serum that was run on each plate. Each sample was run in duplicate.

2.4. In vivo macrophage RCT

J774 cells were radiolabelled with 5 μCi/mL [^{3}H]-cholesterol and 100 μg/mL acetylated low-density lipoprotein for 48 h. Five hundred microliters of cell the suspension containing approximately 1×10^7 cells/mL were injected into the peritoneal cavities of *Cdkal1*$^{fl/fl}$ and *Alb-Cre*:*Cdkal1*$^{fl/fl}$ mice. Plasma samples were collected from the saphenous veins at 48 h. Faeces were collected continuously between 0 and 48 h and were stored at −20 °C until extraction of cholesterol and bile acid. After 48 h, the mice were euthanized by CO_2 inhalation and perfused with cold PBS, and then their livers were harvested. Aliquots (100 mg) of liver tissue were dissolved in 2 mL SOLVABLE (Perkin Elmer, Inc., Waltham, MA, USA) and treated with 0.2 mL 30% hydrogen peroxide. Radioactivity in plasma, liver, and faeces was quantified after lipid extraction and scintillation counting.

2.5. HDL subclass analysis

Lipoproteins were separated using fast protein liquid chromatography (FPLC). Plasma of mice (300 μL) was applied to gel filtration columns (GE Healthcare, Chicago, IL, USA) arranged in AKTApurifier 10 (GE Healthcare). The samples were administered in buffer (0.15 M NaCl, 0.01% EDTA, and 0.2% NaN_3) at a rate of 0.3 mL/min. The solutes passed through the columns were collected on a fraction collector (Frac-950; GE Healthcare) maintained at 4 °C. In each fraction, cholesterol concentration was measured using a colorimetric assay kit (Thermo Fisher Scientific, Waltham, MA, USA). Isolated HDL samples were mixed with 1 mL of dispersant for size measurement. HDL size was measured using dynamic light scattering with a Zetasizer Nano ZS instrument (Malvern Panalytical, Worcestershire, UK). HDL subclasses were defined according to particle size: 8.8–13.0 nm as large HDL, 8.2–8.8 nm as medium HDL, and 7.3–8.2 nm as small HDL. Based on these definitions, HDLs in fractions 19–21, 22–24, and 25–27 of FPLC were considered as large, medium, and small HDLs, respectively.

2.6. Western blotting

Liver tissues were washed in cold PBS and homogenized in PBS containing a protease inhibitor cocktail (Fermentas, Waltham, MA, USA) and phosphatase inhibitor cocktail (Roche, Basel, Switzerland). Protein concentrations of tissue homogenates were determined using a Pierce BCA Protein Assay Kit (Thermo Fisher Scientific). Proteins were separated using SDS-PAGE with a 10% Mini-Protean TGX gel and Mini-

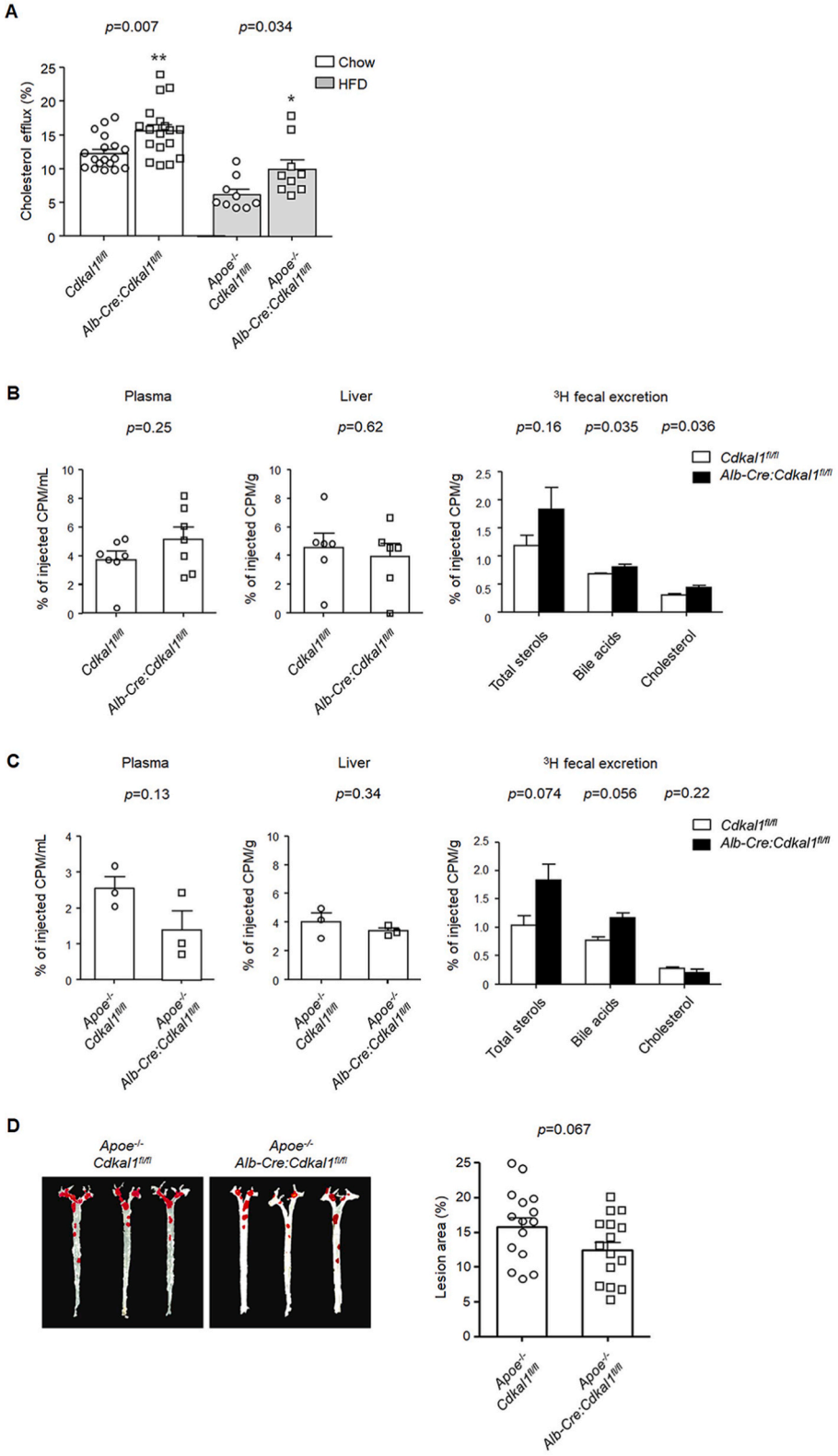

Fig. 2. Effect of Cdkal1 deletion on CEC, macrophage RCT, and aortic atherosclerosis.
(A) J774 cells were plated, radiolabelled with ^{3}H-cholesterol, and incubated with medium containing bovine serum albumin and cyclic adenosine monophosphate (cAMP). The medium was then replaced with another medium and ApoB-depleted male mouse serum. Cholesterol efflux (%) was calculated using the following formula: {^{3}H-cholesterol in medium containing HDL/[^{3}H-cholesterol in medium containing HDL + ^{3}H-cholesterol in cells]} × 100. Each sample was run in duplicate (p = 0.007 and 0.034, respectively; permutation test; n = 9–18 in each group). (B) J774 cells were radiolabelled with ^{3}H-cholesterol and acetylated low-density lipoprotein. Male *Cdkal1*$^{fl/fl}$ and *Alb-Cre*:*Cdkal1*$^{fl/fl}$ mice were injected intraperitoneally with labelled J774 cells. Blood samples were obtained at 48 h, and plasma radioactivity was quantified. Faeces were collected continuously from 0 to 48 h. Mice were euthanized and perfused for harvesting liver and bile. Radioactivity levels in plasma, liver, and faeces were expressed as counts relative to total injected tracer. Faecal bile acids and cholesterol were extracted, and levels were expressed as counts per minute in total faeces (p = 0.035 and 0.036 for % of injected CPM of bile acids and cholesterol, respectively, p = not significant for other comparisons; permutation test; n = 6–7 in each group). (C) Experiments were performed using the same mice fed a high-fat diet for 4 weeks (p = 0.074 and 0.056 for % of injected CPM of total sterols and bile acids, respectively, p = not significant for other comparisons; permutation test; n = 3 in each group). (D) Comparison of atherosclerotic lesions on aortas of *Apoe*$^{-/-}$ and *Apoe*$^{-/-}$*Alb-Cre*:*Cdkal1*$^{fl/fl}$ mice. Male mice were fed high-fat diets for 16 weeks. Oil red O staining of aortas was performed with en face preparation (left). Lesion size was quantified for comparison of the two groups (right) (p = 0.067; permutation test; n = 15 in each group). (For interpretation of the references to color in this figure legend, the reader is referred to the Web version of this article.)

Protean Tetra Cell Mini Trans-Blot module (Bio-Rad Laboratories, Hercules, CA, USA). Proteins were then blotted onto polyvinylidine fluoride membranes (Bio-Rad Laboratories). The blots were incubated with polyclonal anti-rabbit SKP2 (Cell Signaling Technology, Inc., Danvers, MA, USA) or β-actin primary antibodies (Cell Signaling Technology, Inc.) overnight at 4 °C. Incubation was performed with gentle shaking using horseradish peroxidase (HRP)-conjugated secondary antibody, anti-rabbit IgG-HRP, or anti-mouse IgG-HRP (Cell Signaling Technology, Inc.). The immunoreactive bands were visualized using an enhanced chemiluminescence kit (EMD Millipore, Billerica, MA, USA) and densitometric quantification of protein expression was performed using ImageJ. Primary antibodies used for Western blots are described in

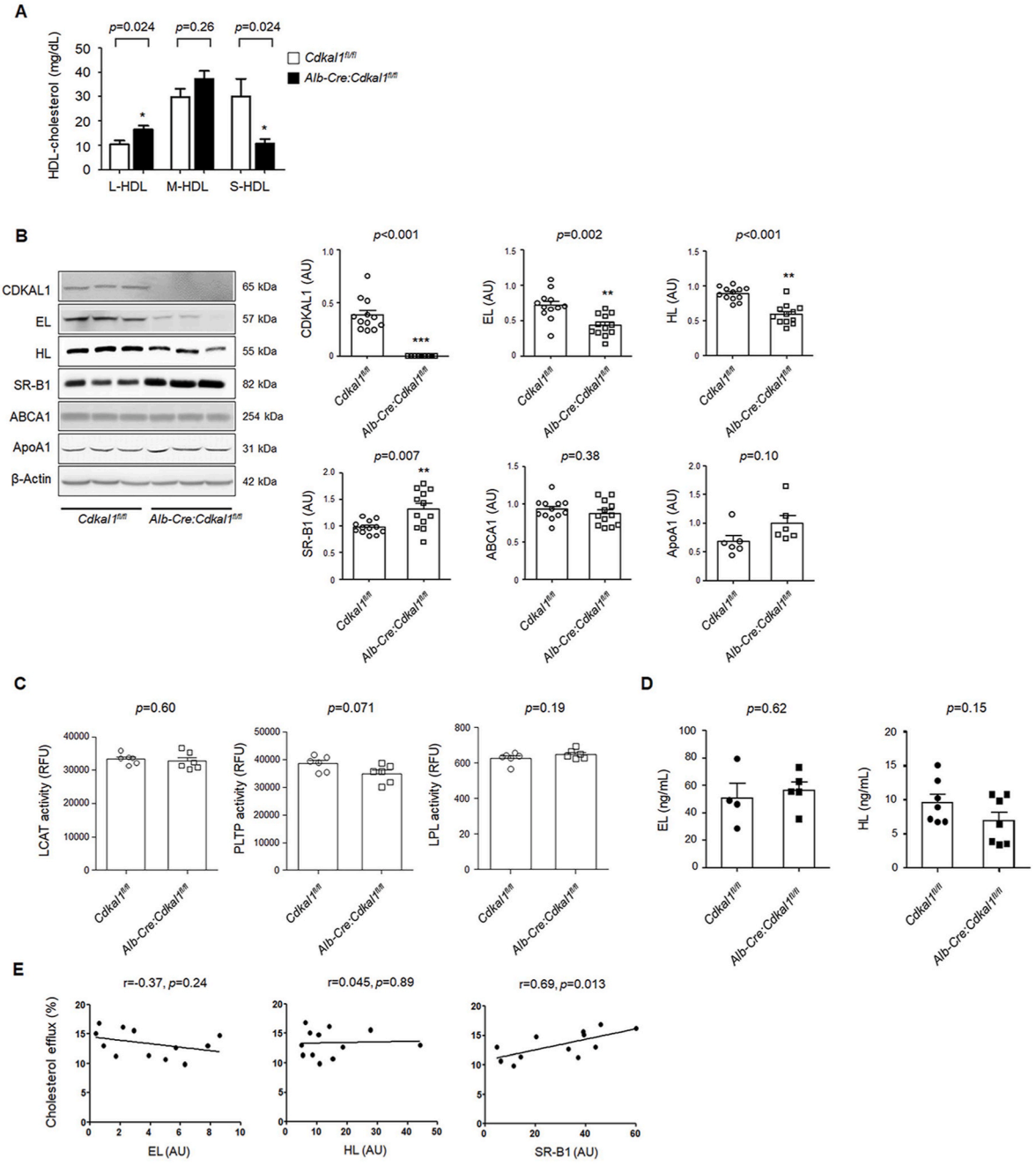

Fig. 3. Effect of Cdkal1 deletion on HDL subclass and regulators of HDL metabolism.
(A) HDL cholesterol in each subclass in male *Cdkal1*$^{fl/fl}$ and *Alb-Cre*:*Cdkal1*$^{fl/fl}$ mice. Lipoproteins were isolated from *Cdkal1*$^{fl/fl}$ (n = 3) and *Alb-Cre*:*Cdkal1*$^{fl/fl}$ mice (n = 5) using fast protein liquid chromatography-mass spectrometry. Cholesterol concentration was quantified at 500 nm absorbance. HDL was isolated from fractions 19–27: fractions 19–21, 22–24, and 25–27 were pooled as large (L-HDL), medium (M-HDL), and small HDL (S-HDL), respectively, and cholesterol concentration was assayed in each subclass ($p = 0.024$ and 0.024 for comparisons of total HDL-C in L-HDL and S-HDL, respectively; Mann-Whitney *U* test).(B) Western blot analysis to evaluate liver proteins participating in HDL metabolism. Proteins extracted from 5-week-old male *Cdkal1*$^{fl/fl}$ and *Alb-Cre*:*Cdkal1*$^{fl/fl}$ mice were separated using electrophoresis followed by immunoblotting. Representative images (left) and densitometric quantification (right) are presented. Cdkal1, EL, HL, SR-B1, ABCA1, and Apo A1 (arbitrary unit) were normalized by β-actin in *Cdkal1*$^{fl/fl}$ and *Alb-Cre*:*Cdkal1*$^{fl/fl}$ mice ($p = 0.001$, 0.002, 0.001, and 0.007 for Cdkal1, EL, HL, and SR-B1, respectively, p = not significant for other comparisons; permutation test; n = 12 in each group). (C) Activities of circulating enzymes involved in HDL metabolism. Activities of LCAT, PLTP, and LPL were measured in male *Cdkal1*$^{fl/fl}$ and *Alb-Cre*:*Cdkal1*$^{fl/fl}$ mice (p = not significant for all comparisons; permutation test; n = 6 in each group). (D) Circulating EL and HL levels were measured using post-heparin plasma from male *Cdkal1*$^{fl/fl}$ and *Alb-Cre*:*Cdkal1*$^{fl/fl}$ mice (p = not significant for all comparisons; permutation test; n = 4–5 in each group). (E) Correlation analysis between CEC and EL, HL, and SR-B1 assayed in western blotting in male *Cdkal1*$^{fl/fl}$ and *Alb-Cre*:*Cdkal1*$^{fl/fl}$ mice ($p = 0.013$ for analysis on SR-B1, p = not significant for other comparisons; Pearson correlation analysis; n = 12). Values are expressed as the mean ± standard error of the mean.

Supplementary Material.

2.7. Enzyme activity assays

Activities of lecithin-cholesterol acyltransferase (LCAT), phospholipid transfer protein (PLTP), and lipoprotein lipase (LPL) were measured using activity assay kits for LCAT (Cat No. 428900; EMD Millipore), PLTP (ab196998; Abcam, Cambridge, UK), and LPL (ab204721; Abcam) according to the manufacturer's instructions.

For LCAT activity, 5-μL aliquots of mouse plasma were incubated at 37 °C with fluorescently labelled cholesterol in assay buffer. After 40 min, 45 μL reaction mixture was added to 135 mL READ agent. The conversion of cholesterol (Em, 470 nm) to cholesteryl ester (Em, 390 nm) was determined using a fluorescence microplate reader at 340 nm excitation. The change in ratio of the two intensities (470/390) was calculated. For PLTP activity, mouse plasma was diluted to 1:10 in PLTP assay buffer, and 10 μL of this solution was used to obtain a signal within the range of the standard curve. Samples were pre-incubated at 37 °C for 10 min with protection from light to stabilize the signal. Fluorescence was measured on a microplate reader at Ex/Em: 464/535 nm in the kinetic mode every 2–3 min for 1–3 h at 37 °C. For LPL activity, mice were infused with 0.2 units of heparin per gram body weight by tail vein injection. Blood was collected 10 min after injection, and plasma was separated. A total of 50 μL reaction mixture was added and pre-incubated at 37 °C for 10 min with protection from light. Output was measured at Ex/Em: 482/520 nm using a microplate reader at 37 °C.

2.8. Enzyme-linked immunosorbent assay (ELISA)

Blood levels of interleukin-1β (IL-1β), endothelial lipase (EL), and hepatic lipase (HL) were quantified using ELISA kits. For IL-1β (Cat No. BMS6002; Invitrogen, Carlsbad, CA, USA), the coated plates were washed twice with washing buffer. After exposure to the medium, the plates were exposed sequentially to each of the biotin-conjugated secondary antibodies. The plates were read at an absorbance of 450 nm, and IL-1β was analysed according to the manufacturer's specifications.

For EL and HL measurement, blood samples were collected after overnight fasting. Ten minutes after intravenous injection of 50 IU heparin/kg, blood was obtained and centrifuged with 3000 rpm for 10 min at 4 °C. Plasma was immediately separated. The levels of EL (Cat No. LS-F4035; LS bio, Seattle, CA, USA) and HL (Cat No. LS-F22470; LS bio) were determined using ELISA kits. Proteins were analysed according to the manufacturer's specification. All assays were performed in duplicate.

2.9. Statistical analyses

All data are presented as the mean ± standard error of the mean. Differences between groups were examined using the Mann–Whitney and permutation tests. Correlations between values were analysed using the Pearson correlation coefficient. Values of $p < 0.05$ were considered statistically significant. All analyses were performed using R version 4.0.4 (R Foundation for Statistical Computing, Vienna, Austria).

3. Results

3.1. Metabolic parameters of liver-specific Cdkal1-deficient mice

Mice with liver-specific Cdkal1 deletion were generated by breeding mice with floxed alleles with those with Cre recombinase (Figure A1, left panel). PCR testing of *Alb-Cre:Cdkal1*$^{fl/f}$ mice revealed appropriate knockdown of the gene (Fig. 1A, middle panel). Body weights from 5 to 16 weeks after birth did not differ between *Cdkal1*$^{fl/fl}$ and *Alb-Cre:Cdkal1*$^{fl/fl}$ mice fed chow diet (Fig. 1A, right panel). Blood levels of glucose, total cholesterol, triglyceride, and low-density lipoprotein-cholesterol were not significantly different in the two groups of mice. In contrast, HDL-C levels tended to be higher in the *Alb-Cre:Cdkal1*$^{fl/fl}$ than in the *Cdkal1*$^{fl/fl}$ mice (76.9 ± 10.4 and 64.4 ± 15.4 mg/dL in each group, respectively; $p = 0.050$) (Fig. 1B). Body weights of male *Apoe*$^{-/-}$*Cdkal1*$^{fl/fl}$ and *Apoe*$^{-/-}$*Alb-Cre:Cdkal1*$^{fl/fl}$ mice were similar (Fig. 1C). Blood levels of glucose and lipids of the two groups (fed high-fat diet) did not differ either (Fig. 1D).

3.2. Effect of Cdkal1 deletion on CEC, RCT, and atherosclerosis

CEC was measured using J774 cells and ^{3}H-cholesterol as described in the Methods section. The experiments were performed on *Cdkal1*$^{fl/fl}$ and *Alb-Cre:Cdkal1*$^{fl/fl}$ mice fed standard chow diets and on *Apoe*$^{-/-}$ and *Apoe*$^{-/-}$*Alb-Cre:Cdkal1*$^{fl/fl}$ mice fed high-fat diets. The CEC of the *Alb-Cre:Cdkal1*$^{fl/fl}$ mice was higher than that of the *Cdkal1*$^{fl/fl}$ mice (15.6 ± 3.9 and 12.3 ± 2.5% in the *Alb-Cre:Cdkal1*$^{fl/fl}$ and *Cdkal1*$^{fl/fl}$ mice, respectively; mean difference 27%; $p = 0.007$), whereas the CEC of the *Apoe*$^{-/-}$*Alb-Cre:Cdkal1*$^{fl/fl}$ mice was higher than that of the *Apoe*$^{-/-}$ mice (9.9 ± 4.1 and 6.1 ± 2.4% in the *Apoe*$^{-/-}$*Alb-Cre:Cdkal1*$^{fl/fl}$ and *Apoe*$^{-/-}$ mice, respectively; mean difference 62%; $p = 0.034$). CEC values were generally lower in mice of the *Apoe*$^{-/-}$ background that were fed the high-fat diets (Fig. 2A).

In vivo RCT experiments using radiolabelled J774 cells in *Cdkal1*$^{fl/fl}$ and *Alb-Cre:Cdkal1*$^{fl/fl}$ mice were performed as described in the Materials and Methods section. On chow diet, the radioactivities of plasma and livers from *Cdkal1*$^{fl/fl}$ and *Alb-Cre:Cdkal1*$^{fl/fl}$ mice were not significantly different. The radioactivities of bile acids (0.81 ± 0.11 and 0.69 ± 0.04% of injected counts per minute [CPM], respectively; mean difference 17%; $p = 0.035$) and cholesterol (0.44 ± 0.10 and 0.31 ± 0.07% of injected CPM, respectively; mean difference 42%; $p = 0.036$) from faeces were higher in the *Alb-Cre:Cdkal1*$^{fl/fl}$ mice than in the *Cdkal1*$^{fl/fl}$ mice, whereas the activities of cholesterol from faeces were similar between the two groups of mice (Fig. 2B). In experiments fed a high fat diet for 4 weeks, the radioactivities of plasma and livers from *Cdkal1*$^{fl/fl}$ and *Alb-Cre:Cdkal1*$^{fl/fl}$ mice did not significantly differ. The activities of total sterols (1.85 ± 0.45 and 1.04 ± 0.27% of injected CPM, respectively; $p = 0.074$) and bile acids (1.13 ± 0.16 and 0.77 ± 0.10% of injected CPM, respectively, $p = 0.058$) from faeces tended to be higher in the *Alb-Cre:Cdkal1*$^{fl/fl}$ mice (Fig. 2C).

To induce atherosclerosis, *Apoe*$^{-/-}$ and *Apoe*$^{-/-}$*Alb-Cre:Cdkal1*$^{fl/fl}$ mice were fed high-fat diets for 16 weeks. The percent areas of atherosclerotic lesions tended to be lower in the *Apoe*$^{-/-}$*Alb-Cre:Cdkal1*$^{fl/fl}$ mice than in the *Apoe*$^{-/-}$ mice (12.4 ± 4.6 and 15.7 ± 5.9%, respectively; $p = 0.067$) (n = 15 in each group; Fig. 2C). Blood levels of interleukin-1β measured in *Cdkal1*$^{fl/fl}$ and *Alb-Cre:Cdkal1*$^{fl/fl}$ mice fed a high-fat diet were 11.5 ± 5.3 and 9.4 ± 3.7 pg/mL, respectively (n = 3 for each group; $p = 0.54$ by permutation test; Supplementary Fig. S2).

3.3. Effects of Cdkal1 deletion on HDL subclass and regulators of HDL metabolism

HDL subclass analysis was performed using fast protein liquid chromatography, and cholesterol concentration and HDL size were measured. Cholesterol concentrations in large HDL particles were significantly higher in the *Alb-Cre:Cdkal1*$^{fl/fl}$ than in the *Cdkal1*$^{fl/fl}$ mice (16.5 ± 3.7 and 10.5 ± 2.5 mg/dL, respectively; $p = 0.024$), whereas its concentrations in small HDL particles were markedly lower in the *Alb-Cre:Cdkal1*$^{fl/fl}$ mice (10.7 ± 4.6 and 30.1 ± 12.4 mg/dL, respectively; $p = 0.024$; Fig. 3A). Western blotting performed using liver tissue revealed significantly reduced EL (0.43 ± 0.15 and 0.71 ± 0.20 arbitrary unit [AU] in the *Alb-Cre:Cdkal1*$^{fl/fl}$ and *Cdkal1*$^{fl/fl}$ mice, respectively; $p = 0.002$) and HL (0.59 ± 0.14 and 0.89 ± 0.10 AU, respectively; $p < 0.001$) as well as elevated SR-B1 (1.32 ± 0.36 and 0.98 ± 0.12 AU, respectively; $p = 0.007$) levels in the *Alb-Cre:Cdkal1*$^{fl/fl}$ mice. Although Apo A1 expression was numerically higher in knockout mice, it was not significant ($p = 0.10$). ATP-binding cassette transporter A1 (ABCA1) expression did not differ between the two groups (Fig. 3B). LCAT, PLTP,

and LPL activities were similar in the *Alb-Cre*:*Cdkal1*$^{fl/fl}$ and *Cdkal1*$^{fl/fl}$ mice, although PLTP activity tended to be lower in the former group (Fig. 3C). ELISA using post-heparin plasma showed that EL (56.8 ± 15.9 and 51.0 ± 21.1 ng/mL in the knockout and control mice, respectively, $p = 0.62$) and HL (4.31 ± 1.41 and 9.68 ± 2.53 ng/mL, respectively, $p = 0.15$) levels were not significantly different between the two mice groups (Fig. 3D). CEC showed significant correlation with SR-B1 expression levels ($r = 0.69$, $p = 0.013$), but not with those of EL or HL (Fig. 3E).

4. Discussion

The major findings of the present study include: 1) CEC and RCT were higher in liver-specific Cdkal1-deficient mice than in *Cdkal1*$^{fl/fl}$ mice. 2) High fat diet-induced aortic atherosclerotic lesions tended to be smaller in *Apoe*$^{-/-}$*Alb-Cre*:*Cdkal1*$^{fl/fl}$ mice than in *Apoe*$^{-/-}$ mice. 3) HDL-C levels tended to be higher in liver-specific Cdkal1-deficient mice, whereas the concentrations of circulating enzymes mediating HDL catabolism were similar in the two groups of mice. 4) EL and HL were downregulated, whereas SR-B1 was upregulated in the liver cells of *Alb-Cre*:*Cdkal1*$^{fl/fl}$ mice, and CEC was positively correlated with SR-B1 expression. 5) Cholesterol concentrations in large HDLs were higher in *Alb-Cre*:*Cdkal1*$^{fl/fl}$ mice than in *Cdkal1*$^{fl/fl}$ mice, whereas cholesterol concentrations in small HDLs were lower. The present study revealed, for the first time, promotion of CEC and RCT in mice with hepatic deletion of Cdkal1, variants of which have been shown to be associated with CEC in a human genome-wide association study (GWAS). In addition, concomitant changes in mediators of HDL catabolism, such as EL and SR-B1, were demonstrated. These results provide evidence that *CDKAL1* could be a therapeutic target for improving RCT and preventing vascular pathology.

There are multiple potential mechanisms to explain how hepatic deletion of Cdkal1 affects HDL metabolism and CEC. EL is mainly synthesized in vascular endothelial cells and has phospholipase activity and HDL affinity [15]. EL cleaves non-esterified fatty acid from HDL-phospholipids and supplies fatty acids for EL-expressing cells. EL promotes remodelling and catabolism of HDL [16]. CEC and RCT were not increased in a previous study by Brown et al. [17], but increased in EL-deficient mice in another report [18]. These studies were not conducted under the same experimental conditions; the macrophages used in the CEC assay and apo-A1 levels in the lipase-deficient mice were different. However, although the conditions in our study were similar to those in the Brown et al. study, our results demonstrated an increase in CEC and RCT in *Cdkal1*$^{-/-}$ mice and a decrease in EL activity. This result indicates that CEC and RCT might be substantially affected by factors other than EL or HL levels, including SR-B1 levels [16]. Furthermore, this finding is concordant with studies that showed low CEC in EL-overexpressed mice [19,20]. In this condition, when SR-B1 function and cholesterol excretion through bile were maintained despite decreased EL function, RCT was not reduced. Interestingly, recent clinical trials have revealed that an anti-EL antibody raised the quantity and functional quality of HDL [21,22]. This is also in line with the higher CEC in *Alb-Cre*:*Cdkal1*$^{fl/fl}$ mice with low EL expression as seen in this study. A previous GWAS showing the relationship between loci near *LIPG* gene (Lipase G, Endothelial Type) coding for EL and CEC [23] substantiates the role of EL on HDL function.

A limitation of our study is that we did not evaluate the role of Cdkal1 on tRNA synthesis in the liver, which is the known function of this protein. It has been reported that tRNA modification is needed in translation during proinsulin synthesis in β cells in the pancreas. In β cell-specific *Cdkal1*$^{-/-}$ mice, such modification was not properly made, and this caused reduction of proinsulin synthesis [10]. In our study, expression of proteins involved in HDL metabolism, such as EL and HL, were significantly lowered. Based on the study mentioned above, it is possible that the tRNA modification needed for translation of EL or HL did not appropriately occur in the liver cells of *Cdkal1*$^{-/-}$ mice. However, we did not conduct experiments to verify this. If further analysis is performed on RNA modification, it may provide clues on more detailed mechanisms [24]. Our animal studies support a role for hepatic Cdkal1 in regulating CEC and RCT. In particular, EL, HL and SR-B1 showed significant differences in expression in mice lacking Cdkal1. The reduction in EL and HL are consistent with the larger HDL particles we observed. Likewise, increased SR-B1 protein in Cdkal1-deficient mice could be certainly contribute to the increased RCT.

The effect of EL on atherosclerosis has been evaluated, but the results were inconsistent. EL deficiency has shown an atheroprotective effect [25], whereas it had no such effect in another study [26]. Conversely, a recent report demonstrated that EL overexpression was atheroprotective [27]. In addition, high circulating EL level was reported to be a predictor of coronary artery disease [28]. However, individuals with *LIPG* variants associated with HDL-C elevation were not protected from atherosclerotic cardiovascular disease [29]. As expression levels of a few molecules other than EL were changed in the present study, the contribution of EL to vascular phenotype is not clear. With regard to RCT promotion, we cannot rule out the possible impact of SR-B1 and other molecules affecting hepatic uptake and bile secretion, respectively. As EL is also involved in degradation of ApoB-containing lipoproteins, their levels can be elevated [22] when EL is inhibited and this can have negative effect on arteries. By contrast, EL overexpression can reduce ApoB-containing lipoprotein levels and potentially inhibit atherosclerosis [16,27]. Although our study identified changes in several molecules including EL, the concentrations of triglycerides and low-density lipoprotein cholesterol in *Alb-Cre*:*Cdkal1*$^{fl/fl}$ mice were not altered. This finding is distinct from those of studies on mice only deficient in EL [25]. It is of note that we need to be cautious not to overinterpret the effect of liver EL on HDL, as plasma EL can be affected by major sources other than the liver.

HL is primarily synthesized by hepatocytes. By hydrolysing triglycerides and phospholipids, HL converts large lipid-rich HDL to smaller poorly-lipidated HDL particles [30]. HL activity decreased in *Alb-Cre*:*Cdkal1*$^{fl/fl}$ mice in our study. HL is known to contribute to degradation of ApoB-containing lipoproteins and convert large HDLs to smaller forms [31]. Based on these roles of HL, degradation of HDL and ApoB-containing lipoproteins could have been inhibited in our *Alb-Cre*:*Cdkal1*$^{fl/fl}$ mice. However, the effects of up- and downregulation of HL on atherosclerosis are unclear. As multiple molecules involved in RCT steps were differentially regulated in *Alb-Cre*:*Cdkal1*$^{fl/fl}$ mice in our study, the actual impact of HL reduction on HDL and vascular phenotype needs to be further investigated.

Upregulation of SR-B1 expression in *Alb-Cre*:*Cdkal1*$^{fl/fl}$ mice might have considerably affected HDL catabolism and CEC in our mice. In addition, increased hepatic cholesterol uptake and RCT via SR-B1 may have influenced atherosclerosis. SR-B1 expression is unchanged in mice deficient in either EL or HL [18,26]. Therefore, the changes in the levels of these proteins in our study might have been the result of independent processes. Although there may be potential interaction between SR-B1 and EL, it has not been clarified yet [20]. Zhang et al. demonstrated that SR-B1 expression in the liver enhances RCT [32], and this could be an essential mechanism underlying the increased RCT seen in the current study. CEC was positively correlated with SR-B1 levels in our study. However, as SR-B1 bi-directionally works on cholesterol efflux as well as cholesterol uptake from HDL [33], the relationship between CEC and SR-B1 levels must be interpreted cautiously. The correlation between the two was found by examining SR-B1 levels in liver cells of *Alb-Cre*:*Cdkal1*$^{fl/fl}$ mice. Thus, as our finding is unrelated to SR-B1 levels of the macrophages we used in the CEC assay, the correlation may not indicate CEC promotion by SR-B1. Collectively, reduction of EL and elevation of SR-B1 in *Alb-Cre*:*Cdkal1*$^{fl/fl}$ mice changed HDL particles and promoted CEC, which may eventually have increased RCT and affected arteries.

Cholesterol concentration of HDL was modestly higher in the large HDL subclass and much lower in the small subclass in *Alb-Cre*:*Cdkal1*$^{fl/fl}$

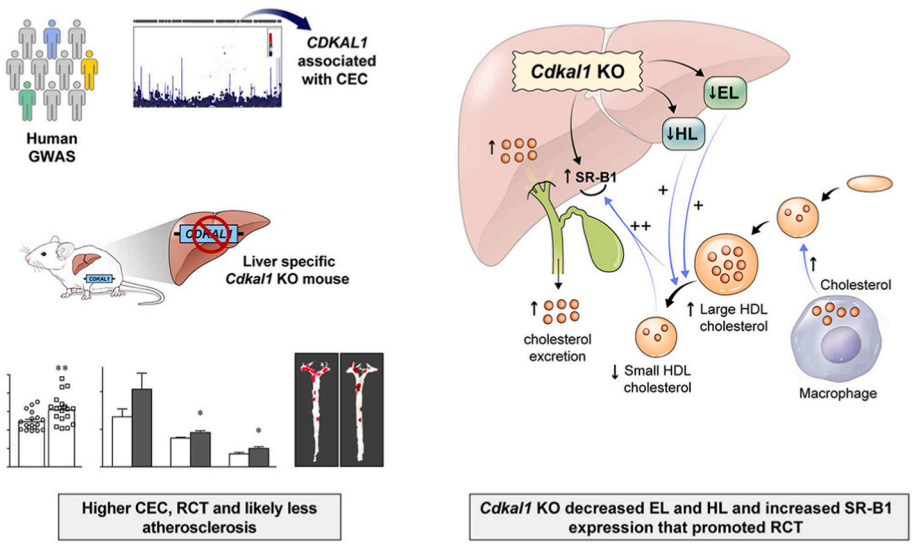

Fig. 4. This study was based on a human GWAS study in which we showed associations between *CDKAL1* variants and CEC. In a mouse model with liver-specific *Cdkal1* deletion, promotion of CEC and RCT and less tendency of atherosclerosis were observed. Regulation of proteins involved in HDL catabolism, including SR-B1, were likely to contribute to these results.

mice than in WT mice. This indicates that large HDL is more abundant and that small HDL is less abundant in *Alb-Cre*:*Cdkal1*$^{fl/fl}$ mice, which may result from decreased HDL degradation due to EL and HL deficiency [34]. This is concordant with a prior study showing that an increase in cholesterol was predominantly seen in large HDL in mice treated with an antisense oligonucleotide against EL [35]. It has been reported that EL-modified small HDL is efficiently taken up by SR-B1, and this promotes RCT [36]. The reduced quantity of small HDL due to EL deficiency in our *Alb-Cre*:*Cdkal1*$^{fl/fl}$ mice might worsen hepatic cholesterol uptake. However, these mice also showed changes in molecules like SR-B1 other than EL and HL, and the net influence of all factors promoted rather than hindered RCT.

Our study has potential limitations. Although Cdkal1 is known to affect tRNA modification and facilitate insulin production in the pancreas, evaluation of such effects was beyond the scope of the present study. However, our study was the first to evaluate the impact of Cdkal1 deletion in liver cells. Furthermore, our study notably started with associations between *CDKAL1* variants and CEC that we discovered in human data. Based on this, we comprehensively evaluated protein expression and enzyme activities influencing CEC and RCT to identify the effects of the association. Although multiple molecules were found to play regulatory roles in the HDL catabolism of our KO mice, we did not further analyse the weight of each molecule's impact. Apo A1 levels in the liver and HDL-C tended to be higher in the *Alb-Cre*:*Cdkal1*$^{fl/fl}$ mice. Although the inter-group difference was not significant, we cannot fully rule out the contribution of these, at least in part, to increased CEC in the knockout mice. In addition, further investigation on adjusted indices, such as CEC per HDL-C, may be helpful to better understand our results.

In conclusion, the current study demonstrated, for the first time, that liver-specific deletion of Cdkal1 promotes CEC and RCT and tends to reduce atherosclerosis. This study verified the effect of *CDKAL1* we previously reported using human CEC and GWAS data. Regulation of proteins involved in HDL catabolism, including SR-B1, contributed to these results (Fig. 4). This study suggests that *CDKAL1* and associated molecules could be targets of intervention for improving RCT and vascular pathology.

Financial support

This work was funded by National Research Foundation of Korea grants funded by the Korean government (grant numbers 2022R1A2C1004946 and 2021R1I1A1A01046940). The funder had no role in the design or conduct of the study; collection, management, analysis, or interpretation of the data; preparation, review, or approval of the manuscript; or decision to submit the manuscript for publication.

CRediT authorship contribution statement

Dan Bi An: Methodology, Validation, Formal analysis, Investigation, Data curation, Writing – original draft, Visualization. **Soo-jin Ann:** Methodology, Validation, Formal analysis, Investigation, Data curation, Writing – original draft, Visualization, Funding acquisition. **Seungmin Seok:** Validation, Formal analysis, Investigation, Data curation. **Yura Kang:** Software, Formal analysis, Visualization. **Sang-Hak Lee:** Conceptualization, Methodology, Resources, Writing – original draft, Writing – review & editing, Visualization, Supervision, Project administration, Funding acquisition.

Declaration of competing interest

The authors declare that they have no known competing financial interests or personal relationships that could have appeared to influence the work reported in this paper.

Acknowledgements

The authors thank Medical Illustration & Design, part of the Medical Research Support Services of Yonsei University College of Medicine, for all artistic support related to this work.

Appendix A. Supplementary data

Supplementary data to this article can be found online at https://doi.org/10.1016/j.atherosclerosis.2023.05.012.

References

[1] Y. Yang, K. Han, S.H. Park, M.K. Kim, K.-H. Yoon, et al., High-density lipoprotein cholesterol and the risk of myocardial infarction, stroke, and cause-specific mortality: a nationwide cohort study in Korea, J Lipid Atheroscler 10 (2021) 74–87, https://doi.org/10.12997/jla.2021.10.1.74.
[2] Y.K. Cho, C.H. Jung, HDL-C and cardiovascular risk: you don't need to worry about extremely high HDL-C levels, J Lipid Atheroscler 10 (2021) 57–61, https://doi.org/10.12997/jla.2021.10.1.57.

[3] M.V. Holmes, F.W. Asselbergs, T.M. Palmer, F. Drenos, M.B. Lanktree, et al., Mendelian randomization of blood lipids for coronary heart disease, Eur. Heart J. 36 (2015) 539–550, https://doi.org/10.1093/eurheartj/eht571.
[4] G.G. Schwartz, A.G. Olsson, M. Abt, C.M. Ballantyne, P.J. Barter, et al., Effects of dalcetrapib in patients with a recent acute coronary syndrome, N. Engl. J. Med. 367 (2012) 2089–2099, https://doi.org/10.1056/NEJMoa1206797.
[5] Q. Zhao, J. Wang, Z. Miao, N.R. Zhang, S. Hennessey, et al., A Mendelian randomization study of the role of lipoprotein subfractions in coronary artery disease, Elife 10 (2021), e58361, https://doi.org/10.7554/eLife.58361.
[6] R.T. George, L. Abuhatzira, S.M. Stoughton, S.K. Karathanasis, D. She, et al., MEDI6012: recombinant human lecithin cholesterol acyltransferase, high-density lipoprotein, and low-density lipoprotein receptor-mediated reverse cholesterol transport, J. Am. Heart Assoc. 10 (2021), e014572, https://doi.org/10.1161/JAHA.119.014572.
[7] B.A. Kingwell, S. Nicholls, E. Velkoska, S.A. Didichenko, D. Duffy, et al., Antiatherosclerotic effects of CSL112 mediated by enhanced cholesterol efflux capacity, J. Am. Heart Assoc. 11 (2022), e024754, https://doi.org/10.1161/JAHA.121.024754.
[8] E.J. Cheon, D.H. Cha, S.K. Cho, H.-M. Noh, S. Park, et al., Novel association between CDKAL1 and cholesterol efflux capacity: replication after GWAS-based discovery, Atherosclerosis 273 (2018) 21–27, https://doi.org/10.1016/j.atherosclerosis.2018.04.011.
[9] H.A. Lee, H. Park, Y.S. Hong, Sex differences in the effects of CDKAL1 variants on glycemic control in diabetic patients: findings from the Korean genome and epidemiology study, Diabetes Metab. J (2022), https://doi.org/10.4093/dmj.2021.0265. Online ahead of print.
[10] F.Y. Wei, T. Suzuki, S. Watanabe, S. Kimura, T. Kaitsuka, et al., Deficit of tRNA (Lys) modification by Cdkal1 causes the development of type 2 diabetes in mice, J. Clin. Invest. 121 (2011) 3598–3608, https://doi.org/10.1172/JCI58056.
[11] F. Oldoni, R.J. Sinke, J.A. Kuivenhoven, Mendelian disorders of high-density lipoprotein metabolism, Circ. Res. 114 (2014) 124–142, https://doi.org/10.1161/CIRCRESAHA.113.300634.
[12] B.T. Palmisano, L. Zhu, J.M. Stafford, Role of estrogens in the regulation of liver lipid metabolism, Adv. Exp. Med. Biol. 1043 (2017) 227–256, https://doi.org/10.1007/978-3-319-70178-3_12.
[13] A.V. Khera, M. Cuchel, M. de la Llera-Moya, A. Rodrigues, M.F. Burke, et al., Cholesterol efflux capacity, high-density lipoprotein function, and atherosclerosis, N. Engl. J. Med. 364 (2011) 127–135, https://doi.org/10.1056/NEJMoa1001689.
[14] M.S. Borja, K.F. Ng, A. Irwin, J. Hong, X. Wu, et al., HDL-apolipoprotein A-I exchange is independently associated with cholesterol efflux capacity, J. Lipid Res. 56 (2015) 2002–2009, https://doi.org/10.1194/jlr.M059865.
[15] S.Y. Choi, K. Hirata, T. Ishida, T. Quertermous, A.D. Cooper, Endothelial lipase: a new lipase on the block, J. Lipid Res. 43 (2002) 1763–1769, https://doi.org/10.1194/jlr.r200011-jlr200.
[16] T. Yasuda, T. Ishida, D.J. Rader, Update on the role of endothelial lipase in high-density lipoprotein metabolism, reverse cholesterol transport, and atherosclerosis, Circ. J. 74 (2010) 2263–2270, https://doi.org/10.1253/circj.cj-10-0934.
[17] R.J. Brown, W.R. Lagor, S. Sankaranaravana, T. Yasuda, T. Quertermous, et al., Impact of combined deficiency of hepatic lipase and endothelial lipase on the metabolism of both high-density lipoproteins and apolipoprotein B-containing lipoproteins, Circ. Res. 107 (2010) 357–364, https://doi.org/10.1161/CIRCRESAHA.110.219188.
[18] J.C. Escolà -Gil, X. Chen, J. Julve, H. Quesada, D. Santos, et al., Hepatic lipase- and endothelial lipase-deficiency in mice promotes macrophage-to-feces RCT and HDL antioxidant properties, Biochim. Biophys. Acta 1831 (2013) 691–697, https://doi.org/10.1016/j.bbalip.2013.01.003.
[19] I. Schilcher, S. Kern, A. Hrzenjak, T.O. Eichmann, T. Stojakovic, et al., Impact of endothelial lipase on cholesterol efflux capacity of serum and high-density lipoprotein, Sci. Rep. 7 (2017), 12485, https://doi.org/10.1038/s41598-017-12882-7.
[20] S. Takiguchi, M. Ayaori, E. Yakushiji, T. Nishida, K. Nakaya, et al., Hepatic overexpression of endothelial lipase lowers high-density lipoprotein but maintains reverse cholesterol transport in mice: role of scavenger receptor class B type I/ATP-binding cassette transporter A1-dependent pathways, Arterioscler. Thromb. Vasc. Biol. 38 (2018) 1454–1467, https://doi.org/10.1161/ATVBAHA.118.311056.
[21] J.E. Le Lay, Q. Du, M.B. Mehta, N. Bhagroo, B.T. Hummer, et al., Blocking endothelial lipase with monoclonal antibody MEDI5884 durably increases high density lipoprotein in nonhuman primates and in a phase 1 trial, Sci. Transl. Med. 13 (2021), https://doi.org/10.1126/scitranslmed.abb0602 eabb0602.
[22] C.T. Ruff, M.J. Koren, J. Grimsby, A.I. Rosenbaum, X. Tu, et al., LEGACY: phase 2a trial to evaluate the safety, pharmacokinetics, and pharamacodynamic effects of the anti-EL (endothelial lipase) antibody MEDI5884 in patients with stable coronary artery disease, Arterioscler. Thromb. Vasc. Biol. 41 (2021) 3005–3014, https://doi.org/10.1161/ATVBAHA.120.315757.
[23] C. Low-Kam, D. Rhainds, K.S. Lo, A. Barhdadi, M. Boulé, et al., Variants at the ApoE/C1/C2/C4 locus modulate cholesterol efflux capacity independently of high-density lipoprotein cholesterol, J. Am. Heart Assoc. 7 (2018), e009545, https://doi.org/10.1161/JAHA.118.009545.
[24] T. Chujo, K. Tomizawa, Human transfer RNA modopathies: disease caused by aberrations in transfer RNA modifications, FEBS J. 288 (2021) 7096–7122, https://doi.org/10.1111/febs.15736.
[25] T. Ishida, S.Y. Choi, R.K. Kundu, J. Spin, T. Yamashita, et al., Endothelial lipase modulates susceptibility to atherosclerosis in apolipoprotein-E-deficient mice, J. Biol. Chem. 279 (2004) 45085–45092, https://doi.org/10.1074/jbc.M406360200.
[26] K.W. Ko, A. Paul, K. Ma, L. Li, L. Chan, Endothelial lipase modulates HDL but has no effect on atherosclerosis development in apoE$^{-/-}$ and LDLR$^{-/-}$ mice, J. Lipid Res. 46 (2005) 2586–2594, https://doi.org/10.1194/jlr.M500366-JLR200.
[27] C. Wang, K. Nishijima, S. Kitajima, M. Niimi, H. Yan, et al., Increased hepatic expression of endothelial lipase inhibits cholesterol diet–induced hypercholesterolemia and atherosclerosis in transgenic rabbits, Arterioscler. Thromb. Vasc. Biol. 37 (2017) 1282–1289, https://doi.org/10.1161/ATVBAHA.117.309139.
[28] X. Yu, J. Lu, J. Li, W. Guan, S. Deng, et al., Serum triglyceride lipase concentrations are independent risk factors for coronary artery disease and in-stent restenosis, J. Atherosclerosis Thromb. 26 (2019) 762–774, https://doi.org/10.5551/jat.46821.
[29] J. Cole, D.M. Blackhurst, G.A.E. Solomon, B.D. Ratanjee, R. Benjamin, et al., Atherosclerotic cardiovascular disease in hyperalphalipoproteinemia due to LIPG variants, J Clin Lipidol 15 (2021) 142–150.e2, https://doi.org/10.1016/j.jacl.2020.12.007.
[30] W. Annema, U.J. Tietge, Role of hepatic lipase and endothelial lipase in high-density lipoprotein-mediated reverse cholesterol transport, Curr. Atherosclerosis Rep. 13 (2011) 257–265, https://doi.org/10.1007/s11883-011-0175-2.
[31] R.S. Rosenson, H.B. Brewer Jr., W.S. Davidson, Z.A. Fayad, V. Fuster, et al., Cholesterol efflux and atheroprotection: advancing the concept of reverse cholesterol transport, Circulation 125 (2012) 1905–1919, https://doi.org/10.1161/CIRCULATIONAHA.111.066589.
[32] Y.Z. Zhang, J.R. Da Silva, M. Reilly, J.T. Billheimer, G.H. Rothblat, et al., Hepatic expression of scavenger receptor class B type I (SR-BI) is a positive regulator of macrophage reverse cholesterol transport in vivo, J. Clin. Invest. 115 (2005) 2870–2874, https://doi.org/10.1172/JCI25327.
[33] M.C. Phillips, Molecular mechanisms of cellular cholesterol efflux, J. Biol. Chem. 289 (2014) 24020–24029, https://doi.org/10.1074/jbc.R114.583658.
[34] M. Tani, K.V. Horvath, B. Lamarche, P. Couture, J.R. Burnett, et al., High-density lipoprotein subpopulation profiles in lipoprotein lipase and hepatic lipase deficiency, Atherosclerosis 253 (2016) 7–14, https://doi.org/10.1016/j.atherosclerosis.2016.08.014.
[35] J. Zhang, Y. Yu, K. Nakamura, T. Koike, A.B. Waqar, et al., Endothelial lipase mediates HDL levels in normal and hyperlipidemic rabbits, J. Atherosclerosis Thromb. 19 (2012) 213–226, https://doi.org/10.5551/jat.11148.
[36] N. Nijtad, H. Wiersma, T. Gautier, M. van der Giet, C. Maugeais, et al., Scavenger receptor BI-mediated selective uptake is required for the remodeling of high density lipoprotein by endothelial lipase, J. Biol. Chem. 284 (2009) 6093–6100, https://doi.org/10.1074/jbc.M807683200.